



IRSTI 34.29.25  
Research article

<https://doi.org/10.32523/2616-7034-2025-151-2-148-168>

## Spectral Characteristics of Spring Wheat Pests Using Hyperspectral Data: Diagnostics and Adaptation Features of Colouring

R.M. Ualiyeva\*<sup>1</sup>, A.V. Osipova<sup>1</sup>, M.M. Kaverina<sup>1</sup>, A.A. Faurat<sup>1</sup>, S.B. Zhangazin<sup>2</sup>

<sup>1</sup>Toraighyrov University, Pavlodar, Kazakhstan

<sup>2</sup>L.N. Gumilyov Eurasian National University, Astana, Kazakhstan

\*Corresponding author: ualiyeva.r@gmail.com

**Abstract.** Using hyperspectral imaging, the spectral characteristics of six pest species (*Chorosoma schillingii*, *Loxostege sticticalis*, *Tettigonia viridissima*, *Chaetocnema aridula*, *Calliptamus italicus*, and *Laodelphax striatella*) associated with spring wheat in northeastern Kazakhstan were investigated for the first time, complementing the few existing studies on this topic. Spectral analysis revealed how these insects reflect, transmit, and absorb light, providing insights for the future application of such data in pest recognition tasks under field conditions. The analysed species exhibited spectral responses within the 500-780 nm range. The analysed species exhibited pronounced spectral responses in the 500-780 nm range, corresponding both to peak reflectance values and the spectral window suitable for diagnostic purposes. A high reflectance coefficient was characteristic of light-coloured and smooth body surfaces, while darker, uneven, and rougher regions tended to scatter light, thereby reducing overall reflectance. Among the studied specimens, *Chorosoma schillingii* showed the highest reflectance due to the combination of a smooth body structure and light pigmentation, which also contributed to strong reflectance in the near-infrared region. The lowest reflectance coefficient was recorded in *Chaetocnema aridula*, explained by the absorption of light by dark pigments. Despite the generally light-coloured exoskeletons of most other species, their reflectance coefficient remained low due to the matte texture of the cuticle. Insect colouration not only aids in camouflage against vegetation but also serves as an adaptation to environmental conditions. Light pigmentation contributes to solar reflectance and prevents overheating, while darker colouration may offer protection against ultraviolet radiation. The variation in colouration across different body parts reflects functional adaptations to specific ecological conditions.

**Keywords:** hyperspectral imaging, spectral characteristics, entomofauna, wheat agrocenosis, pests

Received: 10.04.2025. Accepted: 24.06.2025. Available online: 04.07.2025.

## Introduction

The identification of insect pests plays a key role in ensuring food security, while modern computer vision technologies contribute to accelerating data processing and automating crop inspection for the presence of pests. This opens up new opportunities for the development and implementation of monitoring systems for agricultural lands. In this context, research into the spectral characteristics of pests is essential for training artificial intelligence models capable of automatically detecting and identifying pests in the field [1,2].

Imaging systems have already been applied for the analysis of cuticle structures and phenotypic changes in *Sitophilus oryzae*, classification of *Anastrepha fraterculus*, *Anastrepha obliqua*, *Anastrepha sororcula* Zucchi, *Drosophila melanogaster*, *Drosophila simulans*, *Heliothis virescens*, *Helicoverpa zea*, detection of *Tetramorium caespitum*, *Tetramorium impurum*, and *Trichogramma spp.*, as well as the identification of *Cryptolestes ferrugineus* infestation within wheat kernels [3,4]. Hyperspectral imaging has been studied for detecting *Tetranychus urticae* and *Hemiptera Pseudococcidae* in cotton, describing the integration of alpha taxonomy, mitochondrial DNA, and hyperspectral reflectance profiling of *Cicadellidae*, identifying the pest *Halyomorpha halys*, and taxonomic classification of genera within *Orthoptera* [5-9]. The technology also enables the differentiation of morphologically similar cricket species and the study of insect structural features [10,11].

Hyperspectral imaging represents a rapid and non-destructive method for differentiating infested plants by pest type, as well as a tool for insect classification. However, the broader application of hyperspectral imaging in agriculture for pest identification and assessment of harmfulness requires the expansion of spectral databases of entomofauna. For precise identification and classification, it is essential to analyse insect spectra that reflect their unique optical properties - specifically, the reflection or absorption of light within certain wavelength ranges. This approach allows for the discrimination of even morphologically similar species.

Thus, this study aims to investigate the spectral characteristics of spring wheat pests in northeastern Kazakhstan using hyperspectral imaging. This research is among the few of its kind and the first to provide a detailed examination of the spectral profiles of such pests as *Chorosoma schillingii*, *Loxostege sticticalis*, *Tettigonia viridissima*, *Chaetocnema aridula*, *Calliptamus italicus*, and *Laodelphax striatella*. The obtained data will serve as a foundation for further classification and recognition of these pests through advanced machine learning technologies.

## Materials and research methods

The collection of spring wheat pests was carried out during the crop's vegetation period in 2024 in the main grain-producing areas of Pavlodar Region (northeastern Kazakhstan), specifically in the Zhelezin and Terenkol districts. Pest accounting was conducted using quantitative methods. The target species for this study were *Chorosoma schillingii*, *Loxostege sticticalis*, *Tettigonia viridissima*, *Chaetocnema aridula*, *Calliptamus italicus*, and *Laodelphax striatella* (Figure 1). External appearance of the six pest species selected for analysis; scale bar – 5 mm; all images have a resolution of 300 dpi. The research was conducted at the Laboratory of Biological Research, Toraighyrov University, NPJSC (Pavlodar, Kazakhstan).

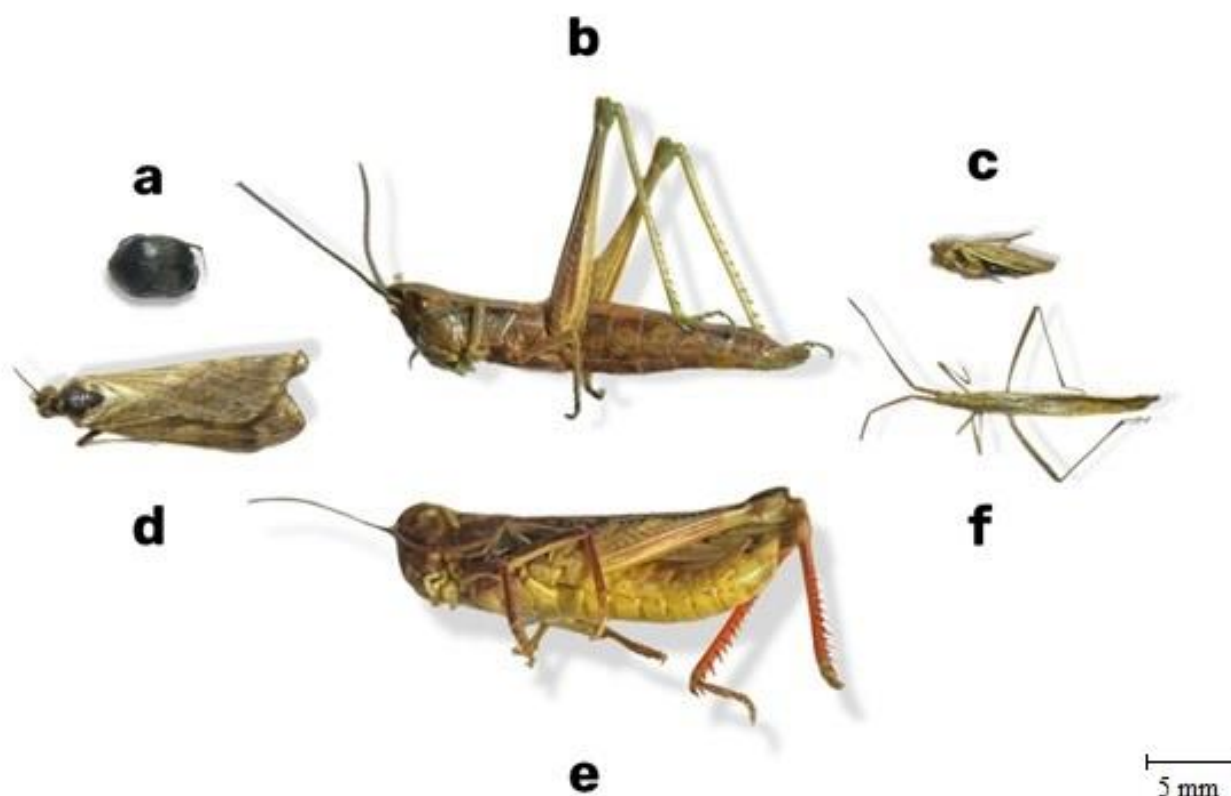


**Figure 1.** Objects of study (**a** – *Chaetocnema aridula*, **b** – *Tettigonia viridissima*, **c** – *Laodelphax striatella*, **d** – *Loxostege sticticalis*, **e** – *Calliptamus italicus*, **f** – *Chorosoma schillingi*)

Hyperspectral imaging of the selected specimens was performed using a FigSpec FS-13 VNIR scanning hyperspectral camera, operating within the 400-1000 nm range, capable of capturing over 250 spectral channels with a spectral resolution of 2.5 nm [12]. Preliminary visual quality control of the acquired hyperspectral images was carried out in the Breeze software environment, with further data processing implemented using the IDL programming language. A PCA (Principal Component Analysis) model was constructed using machine learning methods [13,14] in the Pixel Explore module, based on all image pixels. Five principal components were used for the analysis, collectively explaining 94.6% of the total variance in the spectral data (PC1 – 58.2%, PC2 – 21.4%, PC3 – 8.7%, PC4 – 4.1%, PC5 – 2.2%). These values allow for a reliable interpretation of the observed differences between species in the PCA plots (Figures 2 and 3). The dataset included spectral plots (Raw Spectrum), variance scatter plots, and a hyperspectral image based on maximal variance. For each insect species, between 15 and 25 individuals were selected (*Anisoplia austriaca* – 20, *Anisoplia agricola* – 18, *Phorbia fumigata* – 15, *Trigonotylus ruficornis* – 25, *Phyllotreta vittula* – 22, *Haplothrips tritici* – 20). The collection was carried out in the morning and early afternoon hours (from 8:00 AM to 1:00 PM) under predominantly clear weather conditions. Lighting conditions during hyperspectral imaging were carefully recorded: 82% of the samples were captured under direct sunlight, and 18% under diffuse light on overcast days.

For statistical analysis, modeling, and data visualisation, SigmaPlot 15.0 was used with Python programming language support, integrated with Microsoft Excel for streamlined data import and analysis. Spectral data were statistically processed using analysis of variance (ANOVA) and descriptive statistics methods.

Before conducting the ANOVA, the main assumptions were tested: normality was assessed using the Shapiro-Wilk test ( $p > 0.05$  for all groups), and homogeneity of variances was evaluated using Levene's test ( $p > 0.05$ ) [15,16]. All obtained p-values are presented in Table 2.

Minimum and Maximum Reflectance are calculated using the formulas:

$$R_{\min} = \min (R_1, R_2, \dots, R_n)$$
$$R_{\max} = \max (R_1, R_2, \dots, R_n)$$

where  $R_{\min}$  and  $R_{\max}$  are the minimum and maximum reflectance values within the sample;  $R_1, R_2, \dots, R_n$  are the individual reflectance measurements; and  $n$  is the total number of measurements.

Mean Reflectance represents the average intensity of reflected light within the analysed spectral range and characterises the general reflectance level of the object. It is calculated as:

$$\mu = \frac{1}{n} \sum_{i=1}^n R_i$$

Where  $R_i$  is the reflectance value for the  $i$ -th measurement, and  $n$  is the total number of measurements [17, 18].

Standard Deviation quantitatively indicates the dispersion of reflectance values from the mean, allowing for the assessment of how statistically distinguishable the spectra are. It is calculated using the formula. It is computed as:

$$\sigma = \sqrt{\frac{1}{n} \sum_{i=1}^n (R_i - \mu)^2},$$

where  $\mu$  is the mean reflectance,  $R_i$  is the reflectance value of the  $i$ -th measurement, and  $n$  is the total number of measurements.

Before each imaging session, the camera was calibrated using a white reference standard (Spectralon 99%) and a dark frame (with the lens covered). The distance between the lens of the Figspec FS-13 hyperspectral camera and the specimen was 20 cm. Illumination was provided by natural daylight.

Coefficient of Variation (CV) expresses the degree of variability and enables the evaluation of how variable the insect spectra are relative to their mean value. It is calculated using the formula:

$$CV = \frac{\sigma}{\mu} \times 100,$$

where  $\sigma$  is the standard deviation and  $\mu$  is the mean reflectance.

Rate of Change (RoC) is a dynamic parameter describing the rate of reflectance coefficient variation over time. It helps assess the temporal dynamics of spectral properties in a single subject. The formula is:

$$\Delta R = \frac{R_2 - R_1}{T_2 - T_1},$$

where  $R_1$  and  $R_2$  are reflectance values at time points  $T_1$  and  $T_2$ , respectively.

Delta Reflectance ( $\Delta R$ ) indicates the difference between maximum and minimum reflectance values within a specific spectral range or between two measurement conditions:

$$\Delta R = R_{\max} - R_{\min}$$

where  $R_{\min}$  and  $R_{\max}$  are the minimum and maximum reflectance values within the sample.

Spectral Bandwidth refers to the width of the spectral range in which significant changes in reflectance occur. It helps to identify regions where the object exhibits distinct optical properties, such as maximum absorption or reflection. The overlap or separation of spectral bands across different species or conditions can be used to detect statistically significant differences. It is calculated using the formula:

$$SB = \lambda_{\max} - \lambda_{\min}$$

where  $\lambda_{\min}$  is the minimum wavelength, and  $\lambda_{\max}$  is the maximum wavelength.

Spectral Skewness describes the asymmetry in the distribution of reflectance and absorption values. It is calculated using the formula:

$$SS = \frac{1}{n} \sum_{i=1}^n \left( \frac{R_i - \mu}{\sigma} \right)^3,$$

where  $\sigma$  is the standard deviation,  $\mu$  is the mean reflectance,  $R_i$  is the reflectance value for the  $i$ -th measurement, and  $n$  is the total number of measurements.

The calculated parameters, such as minimum and maximum reflectance, mean reflectance, standard deviation, and coefficient of variation, enable a quantitative assessment of the spectral characteristics of the studied objects and allow for the identification of differences among them. Methods such as Principal Component Analysis (PCA), along with metrics like rate of change and delta reflectance, provide a more comprehensive understanding of the variability in spectral features. These data form the basis for the further development of classification models and can be employed for effective detection and monitoring of pests in agricultural fields, thereby contributing to the enhancement of crop protection systems.

## Results

The images present the spectral characteristics of insects obtained via hyperspectral imaging [19-22]. Each insect specimen and its corresponding spectral curve are assigned matching numbers; for instance, the first red line in the Raw Spectrum graph corresponds to specimen number one in the hyperspectral image [23]. *Chaetocnema aridula* is a small, oval-shaped insect

measuring 2-3 mm in length (Figure 1). Its body exhibits a shiny surface with a greenish-bronze sheen. The elytra, pronotum, and legs are uniformly black.

According to the Raw Spectrum graph, the insect demonstrates low reflectance due to its dark colouration, which absorbs a significant portion of incident light (Figure 2). A reflection peak is observed in the 500-750 nm range, while a decline in intensity beyond 750 nm indicates reduced chitin reflectivity in the near-infrared region, which is typical of dark-coloured surfaces. The highest reflectance is recorded in the first sample, attributed to the smoother surface texture of the elytra.

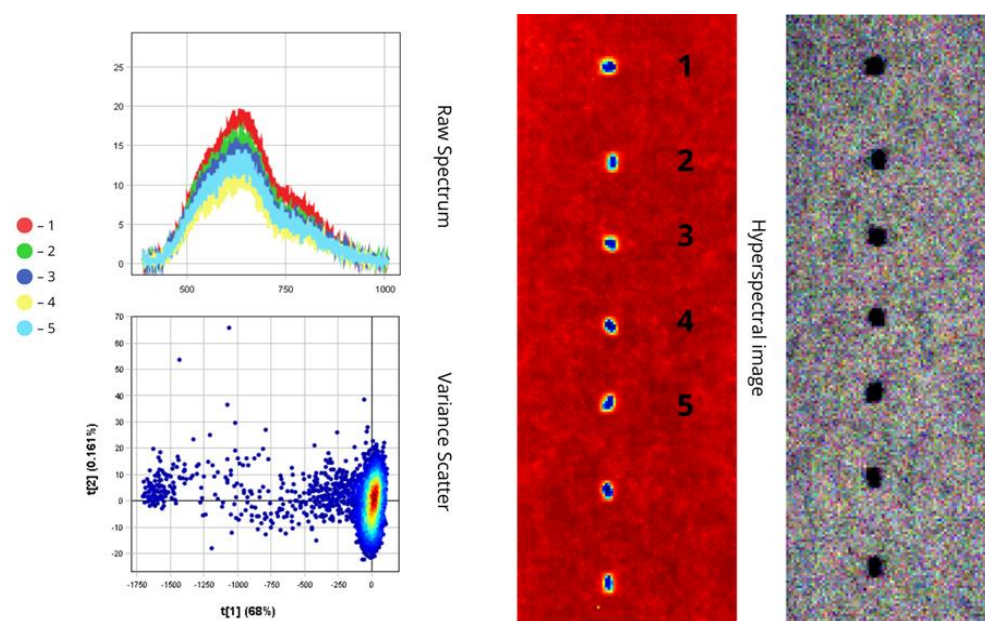


**Figure 2.** Spectral characteristics of *Chaetocnema aridula*

In contrast, the lowest reflectance is observed in the fourth sample, which was positioned with its abdomen facing upward, thereby reducing the amount of reflected light. The Variance Scatter Plot for *Chaetocnema aridula* displays low data density, which can be explained by the insect's small size and its morphological and spectral characteristics. Due to the limited number of pixels captured during hyperspectral imaging, less spectral information is collected. Moreover, the presence of pigments that absorb light within specific wavelength ranges reduces the overall spectral variability, resulting in a sparser distribution in the scatter cloud.

The imago of *Tettigonia viridissima* reaches a length of 20-25 mm, with colouration ranging from green and yellow to pinkish-yellow (Figure 1). The head features a well-defined, laterally compressed vertex and is equipped with antennae. The male's forewings possess a stridulatory organ, consisting of a mirror, a transparent resonating membrane, and a stridulatory section. In the Raw Spectrum graph, the highest reflectance is observed in the first sample, where the selected region includes the wings (Figure 3).



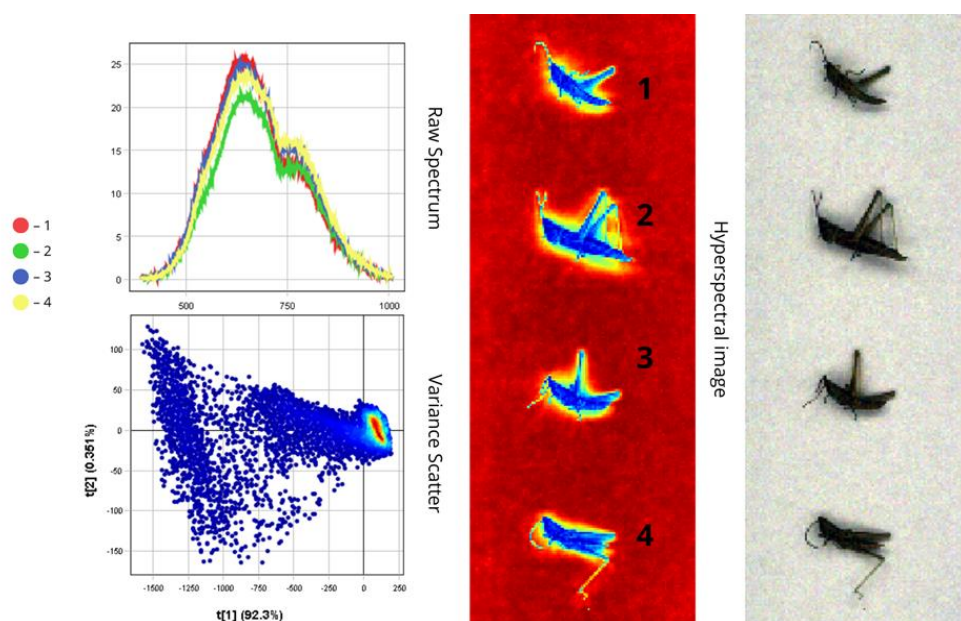


**Figure 3.** Spectral characteristics of *Tettigonia viridissima*

The wing membrane reflects more light than the insect's chitinous exoskeleton. The lowest reflectance is recorded in the second sample, where the wings are not visible in the image. The size and position of the wings enhance the overall spectral intensity due to light scattering. The spectral peak is observed in the 500-750 nm range, while the intensity decrease beyond 750 nm indicates a reduction in chitin reflectance in the near-infrared spectrum. In the Variance Scatter Plot, the high point density observed in the scatter cloud can be attributed to the uniformity of the cuticular structure and the larger body size of *Tettigonia viridissima*. With a greater surface area, more spectral data is collected from various regions, leading to an increase in point density. The spectral characteristics remain relatively uniform due to the consistency in surface structure across the insect's larger body.

*Chorosoma schillingi* measures 11-15 mm in length and has a slender, yellow-green body (Figure 1). The fifth sample exhibits the highest intensity due to its lighter colouration and less dense chitinous exoskeleton, which allows more light to be reflected (Figure 4). In contrast, the first sample shows the lowest intensity because of its rougher body surface, which causes more light scattering. The spectral graph shows an intensity peak in the 500-780 nm range, indicating limited reflection in the near-infrared spectrum. In the Variance Scatter plot, the moderate point density is associated with the insect's narrow body. A narrower body provides a smaller surface area, which restricts the amount of spectral data collected. This results in an average point density, as spectral variability is less pronounced due to the smaller volume of data. Additionally, the insect's narrow shape may contribute to more localised spectral differences, such as segmentation or structural variations, which increase data spread and reduce overall density.

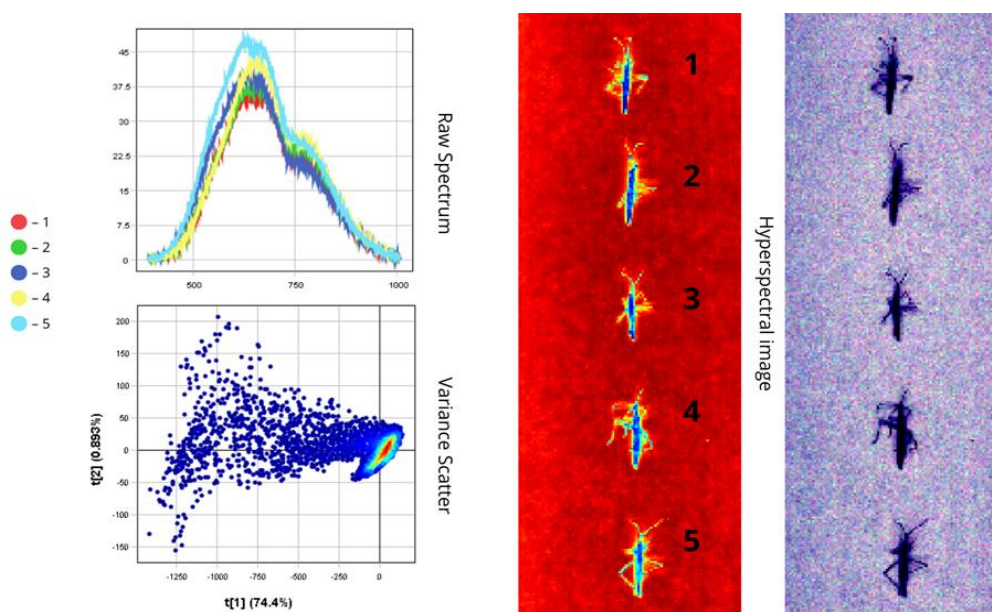


**Figure 4.** Spectral characteristics of *Chorosoma schillingii*

*Loxostege sticticalis* has light brown forewings with a dark brown pattern and greyish-brown hindwings (Figure 1). It features a head with compound eyes and simple thread-like antennae, measuring 17-19 mm in length. The spectral intensity peak falls within the 500-780 nm range (Figure 5). The first sample has the lowest reflection coefficient due to its darker, brownish colouration. In contrast, the second sample, which has a lighter body, exhibits the highest reflection coefficient. According to the Raw Spectrum graph (Figure 5), the head reflects significantly less light than the wings. The wings exhibit a higher reflection coefficient than other body parts due to their structure, which allows them to reflect more incident light rather than absorb it. Wing venation and fine scales, characteristic of *Lepidoptera*, contribute to this effect. Scales on the wings can be pigment-based, determining colouration, or structural, producing optical effects such as iridescence or sheen through light interference, which enhances reflectivity. Some scales possess microscopic structures that interact with light, causing reflection and refraction, thereby significantly increasing wing reflectivity even in the absence of bright pigments. The wing surface, covered in scales, is relatively smooth at the microscopic level, further enhancing light reflection. The light-coloured wings of *Loxostege sticticalis* enhance reflectivity despite the presence of brown pigments. The thin and transparent wing membrane also contributes to a higher reflection coefficient than other body parts. High reflectivity may be an adaptive trait, aiding in temperature regulation by reflecting sunlight and providing camouflage by blending with bright surroundings, such as sunlit grass.



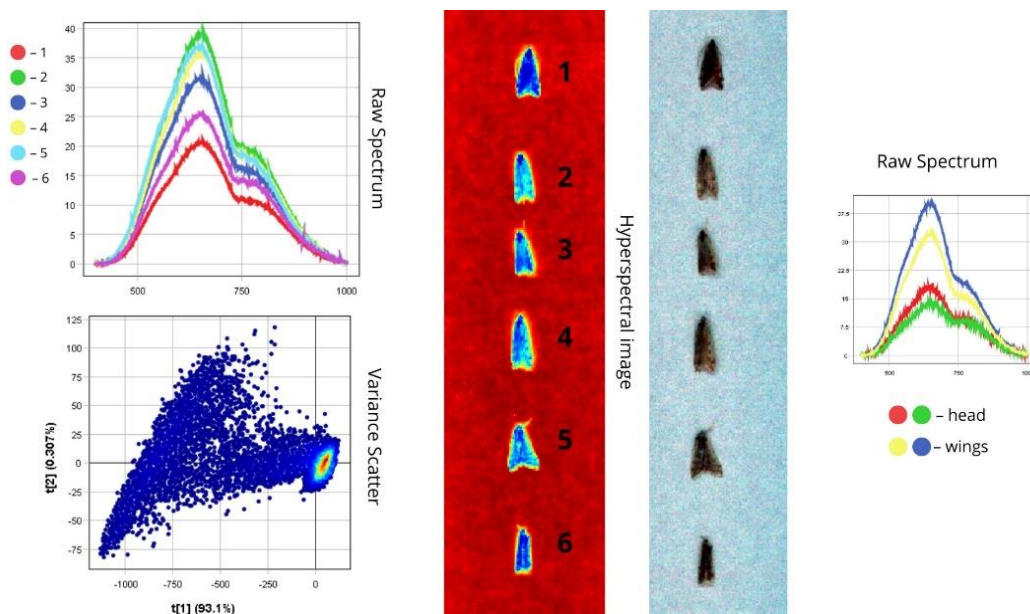


**Figure 5.** Spectral characteristics of *Loxostege sticticalis*

*Calliptamus italicus* ranges in length from 20 to 25 mm and is predominantly brown and yellow-brown in colour (Figure 1). The spectral graph shows the highest reflection coefficients in the third and fourth samples, while the first, second, and fifth samples have the lowest (Figure 6). The third and fourth samples have visibly yellow abdomens, whereas the others are positioned at different angles, making them appear darker. The intensity peak occurs within the 550-750 nm range, decreasing in the near-infrared spectrum.

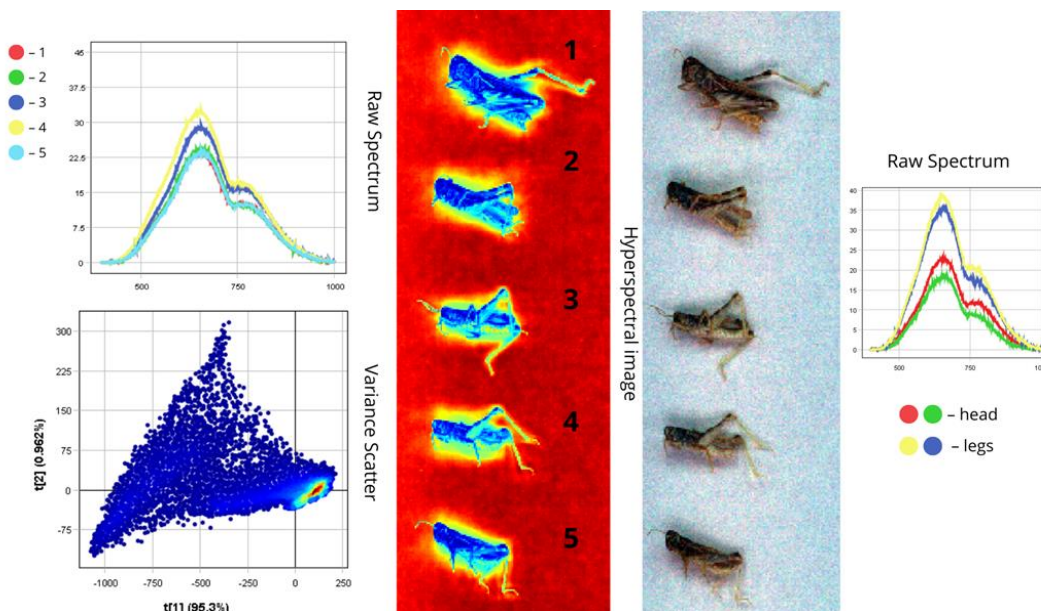


**Figure 6.** Spectral characteristics of *Calliptamus italicus*

The Raw Spectrum graph displays spectra from the head and limbs. The head is darker than the abdomen and limbs due to the presence of pigments such as melanin in the cuticle. Dark pigments absorb more light, reducing reflectivity. This darker colouration may provide camouflage and protection against ultraviolet radiation, both crucial for survival. Additionally, lower reflectivity could result from the denser chitin composition of the head. In contrast, the limbs are lighter in colour, containing fewer pigments, which results in higher reflectivity. This lighter colouration helps reflect sunlight, preventing overheating during active movement.

Imago *Laodelphax striatella* measures 4 mm in length (Figure 1). Males have yellow bodies, while females are black-brown with black-striped patterns. Their transparent wings feature a brownish smear on the inner side in females or a partially smoky appearance in males. Due to this sexual dimorphism, the spectra of males and females may differ based on pigment composition. The first sample has the lowest reflection coefficient, while the second and third samples have the highest (Figure 7). Samples positioned with their abdomens facing upward may show lower intensity, whereas those with wings facing upward exhibit higher reflectivity within the same sex. The spectral intensity peak occurs within the 550-750 nm range. In the Variance Scatter plot, the low point density is attributed to the insect's small size, which limits the number of spectral data points captured.

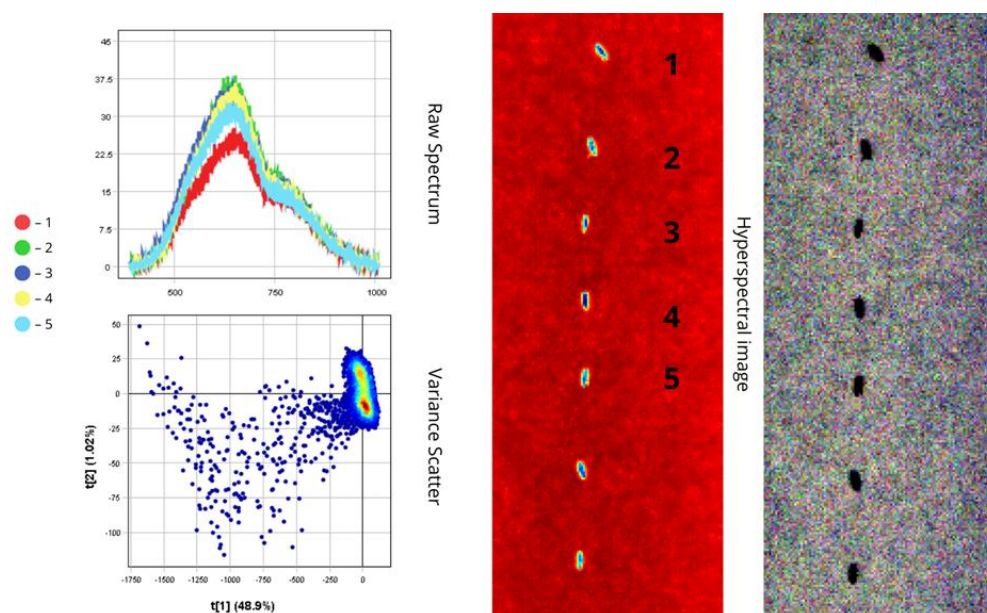


**Figure 7.** Spectral characteristics of *Laodelphax striatella*

The generalised spectral characteristic data are presented in Table 1. The statistical analysis of the data allowed for the identification of key patterns in the spectral characteristics (Table 2) of the insects, the assessment of their variability and stability, and the clear and informative visual presentation of the results.

The highest maximum reflectance is observed in *Chorosoma schillingi* due to its light pigment and in *Loxostege sticticalis* due to the reflective ability of the wing membrane, while the lowest

is seen in *Chaetocnema aridula* due to its dark pigment. Mean Reflectance simplifies complex spectral data into a single numerical value, making it easier to compare between individuals or species. *Chaetocnema aridula* has the lowest mean value, which corresponds to the lowest reflection intensity among all the samples. *Laodelphax striatella* shows the highest mean value due to the presence of light pigments and nearly uniform reflectivity across the samples of the species.

Table 1

## Spectral characteristics of insects

№	Species	Body part	Wave lenght (nm)	Reflection coefficient (%)
1	<i>Chaetocnema aridula</i>	Body	500-750	10-20
2	<i>Tettigonia viridissima</i>	Body	500-750	20-25
3	<i>Chorosoma schillingi</i>	Body	500-780	35-45
4	<i>Loxostege sticticalis</i>	Body	500-780	20-40
		Head	500-750	15
		Wings	500-780	30-38
5	<i>Calliptamus italicus</i>	Body	550-750	22,5-35
		Head	500-750	20-25
		Legs	500-750	35-40
6	<i>Laodelphax striatella</i>	Body	550-750	22,5-37,5

The Standard Deviation values among the presented samples are low, confirming the reproducibility of measurements within a species. For instance, in *Chaetocnema aridula*,  $\sigma = 2.89\%$  for reflection at 750 nm, meaning most values lie within  $\pm 2.89\%$  of the mean. High values suggest measurement errors or biological variability, with a greater diversity of characteristics within a species. For samples with high values (e.g., 15%), additional tests such as the t-test should be conducted. This indicator also allows for the assessment of variability within a species: if the reflection  $\sigma$  increases sharply over the course of a year, it may indicate adaptation to new environmental conditions.

*Tettigonia viridissima* and *Chorosoma schillingi* have low Coefficient of Variation values, indicating high reproducibility of data. *Chaetocnema aridula*, *Loxostege sticticalis*, and *Laodelphax striatella* exhibit moderate variability, linked to biological heterogeneity among the samples, such as age differences and cuticle condition. Stable species demonstrate low RoC values, indicating the stability of their optical properties. *Loxostege sticticalis* has a primary RoC = 15, a relatively high rate of change. Combined with a high  $\Delta R$  (20%), this suggests significant variability in reflectance, possibly due to age differences within the sample and varying cuticle conditions (e.g., moulting or damage). *Calliptamus italicus* shows a sharp increase in RoC = 15 in the head region, where the colouration significantly differs from the rest of the body.

Stable species also exhibit lower  $\Delta R$  under changing conditions. The  $\Delta R$  value of 5% in *Tettigonia viridissima* indicates the species' stability. Values of 10-20% exceed the natural

fluctuation typical of stable populations. In a small sample, this is not significant, as random fluctuations distort the result. Elevated  $\Delta R$  and  $\sigma$  values in some species suggest the need to account for external factors.

**Table 2**

**Statistical analysis of spectral reflection coefficients**

№	Species	Body parts	Min Reflectance	Max Reflectance	Mean Reflectance	Standard Deviation	Coefficient of Variation	Median	RoC	Delta Reflectance	Shapiro-Wilk (p)	Levene's Test (p)
1	<i>Chaetocnema aridula</i>	Body	10	20	15	2,89	19,25	15	–	10	0,15	0,30
2	<i>Tettigonia viridissima</i>	Body	20	25	18,4	1,44	7,84	18,4	–	5	0,55	0,70
3	<i>Chorosoma schillingi</i>	Body	35	45	32,4	2,89	8,91	32,4	–	10	0,08	0,60
4	<i>Loxostege sticticalis</i>	Body	20	40	30	5,77	19,25	30	15	20	0,03	0,02
		Head	15	15	15	0	0	15	19	0	1,00	–
		Wings	30	38	34	2,31	6,79	34	4	8	0,40	0,80
5	<i>Calliptamus italicus</i>	Body	22,5	35	26,5	3,61	13,62	26,5	4	12,5	0,07	0,25
		Head	20	25	22,5	1,44	6,42	22,5	15	5	0,65	0,90
		Legs	35	40	37,5	1,44	3,85	37,5	11	5	0,75	0,85
6	<i>Laodelphax striatella</i>	Body	22,5	37,5	33	4,33	13,12	33	–	15	0,04	0,10

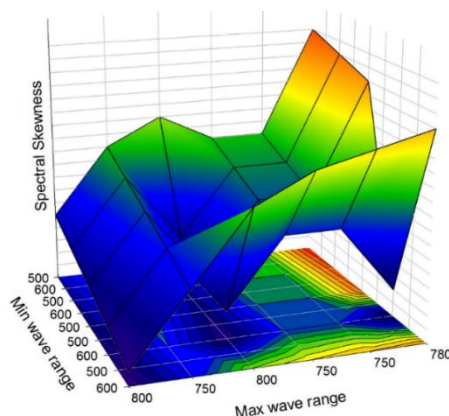
Overall, all species exhibit nearly identical Spectral Bandwidth values due to the similar organisation of the chitinous exoskeletons, as they belong to the same class. Among the samples, a slight positive skew in Spectral Skewness is observed in *Chorosoma schillingi*, *Calliptamus italicus*, and *Laodelphax striatella*, which is attributed to the presence of pigments that are rare in the sample but intense. No asymmetry is observed in the remaining species (Table 3). A positive value of Spectral Skewness indicates a shift of the reflectance spectrum towards the long-wavelength region, which may suggest the predominance of dark pigments. Conversely, negative skewness indicates stronger reflectance in the short-wavelength range, implying the presence of pigments that more effectively reflect blue and green light.

Table 3

## Statistical analysis of the spectrum range

Nº	Species	Body parts	Min	Max	Spectral Bandwidth	Spectral Skewness
1	<i>Chaetocnema aridula</i>	Body	500	750	250	0
2	<i>Tettigonia viridissima</i>	Body	500	750	250	0
3	<i>Chorosoma schillingi</i>	Body	500	750	250	0,390
4	<i>Loxostege sticticalis</i>	Body	500	780	280	0
		Head	500	750	250	–
		Wings	500	780	280	0,312
5	<i>Calliptamus italicus</i>	Body	550	750	200	0,408
		Head	500	750	250	0
		Legs	500	750	250	-0,204
6	<i>Laodelphax striatella</i>	Body	550	750	200	0,618

The statistical data processing results were visualised using SigmaPlot 15.0. The data in Figure 8 are presented in a colour gradient, covering the wavelength range indicators and spectral skewness. Darker areas (dark blue) represent negative skewness values, indicating a leftward shift in the distribution. The gradual transition to yellow-orange colours reflects positive skewness values, suggesting a rightward shift in the distribution. This allows for the visualisation of differences in spectral shape or data distribution, where brightness and colour gradation help easily identify areas with varying degrees of asymmetry.



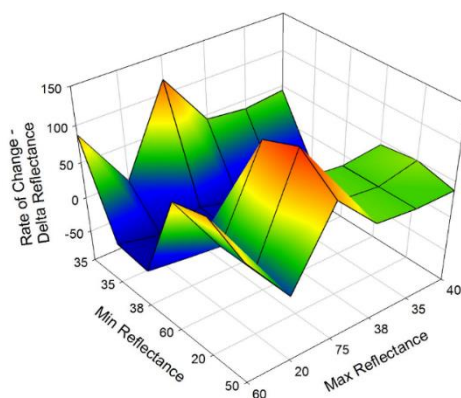
Note: x-axis – maximum wavelength value; y-axis – minimum wavelength value; z-axis – spectral skewness

Figure 8. Wavelength indicators (nm) and spectral skewness

The data in Figure 9, presented in a colour gradient, reflect the values of the reflection coefficient, rate, and delta of reflection. The dark blue areas indicate higher reflectivity of the studied objects, as well as a range with lower values of rate and delta of reflection. This may suggest stable or slow reflection processes in the studied samples. The orange-red areas



demonstrate lower values of the reflection coefficient, which are associated with higher values of the rate and delta of reflection, respectively.



*Note:* x-axis – maximum reflection coefficient value; y-axis – minimum reflection coefficient value; z-axis – rate and delta of reflection

**Figure 9.** Reflection coefficient, rate, and delta indicators

These areas may indicate changes in the exoskeleton structure or the chemical composition of the insect body or its parts, leading to rapid variations in the reflection characteristics, which are displayed in the colour gradient of hyperspectral images. The colour gradient serves as a tool for quickly identifying areas with unique characteristics.

### Discussion

This work represents the first study of the phenotypic traits, where spectral characteristics of pest entomofauna in wheat agrocenoses were described using hyperspectral imaging and computer vision technologies. The imaging demonstrated the high sensitivity of the method to differences in the reflectivity of the exoskeleton. The variation in intensity reflects the variability between different body parts and morphological features of the individuals [24-26], such as pigmentation, density, chitin structure, and age. Despite the differences of each individual sample, the spectral curves exhibit similar intensity and wavelength for each species, which forms the basis for their identification [27,28]. The obtained spectral signatures provide a solid foundation for developing machine learning algorithms that enable automatic classification of pests based on their unique reflectance spectra [29,30]. Future work will focus on building and validating models such as PLS-DA, SVM, and neural networks using the presented set of spectral profiles to create effective pest monitoring systems [31,32].

The study results show that reflectivity decreases with the presence of a larger amount of dark pigment in the cuticle. Higher reflectivity is observed in insects with lighter body coverings, such as *Laodelphax striatella* with yellow pigment and *Chorosoma schillingii* with green pigment. This supports previous research where it was found that insects with white, red, orange, and yellow colouration exhibit high reflectivity, a property also observed in some green species [12].

The combination of pigment composition, surface smoothness of the chitin, and cuticle density is also crucial. Insects with lighter colouration and a matte or rough body surface will

exhibit lower reflectivity. Among all the studied insects, *Loxostege sticticalis* spans the near-infrared spectrum due to the effective reflection of light from its smooth, light-coloured wing surface at the micro level. The wings are covered with microscopic scales that act as a diffraction grating, causing light interference. This creates iridescence. Keratin and chitin in the wings form translucent layers that reflect light. Bright reflection may be an adaptation: it aids in camouflage among foliage, attracts mates, and prevents overheating of the wings. The bodies of insects are typically covered with a matte cuticle with roughness that scatters light, while their legs and antennae have setae that absorb light, leading to the lowest reflectivity in these parts of the body. Additionally, the heads of insects generally contain more dark pigments than other body parts, which may serve as protection against ultraviolet radiation, as seen in *Calliptamus italicus*. Overall, insects with a predominance of melanin colouration exhibit the highest peak in the visible range (500-750 nm), with little or no reflection in the near-infrared spectrum. The combination of small size, dark colouration, and matte covering results in the lowest reflectivity coefficient, as observed in *Chaetocnema aridula*.

Based on the statistical analysis, the most stable species is *Tettigonia viridissima*, with the least variation observed within the sample. The most significant intra-species differences are found in *Loxostege sticticalis*, due to both the small number of objects in the sample and the greater diversity of colouration and wing structure, which increases variability. The study of spectral characteristics opens up opportunities for the application of technology [33,34] in precise, rapid, and non-invasive research on the morphology, taxonomy of insects, and pest detection in fields.

## Conclusion

In this study, the spectral characteristics of the wheat pests *Chorosoma schillingii*, *Loxostege sticticalis*, *Tettigonia viridissima*, *Chaetocnema aridula*, *Calliptamus italicus*, and *Laodelphax striatella* were described for the first time. The obtained data provide insights into how insects interact with light, reflecting, transmitting, and absorbing it, opening new opportunities for their classification and efficient application in agricultural practices.

The spectral characteristics of insects not only help create databases for their identification but also reveal the adaptive features of their colouration in response to light exposure. Light colouration can help prevent overheating by reflecting sunlight, while dark colouration protects against ultraviolet radiation. The diversity of colours on different parts of the insect body is a result of such ecological adaptations.

The highest reflectance was demonstrated by the *Chorosoma schillingii* sample, which is related to its smooth structure and light colouration, while the lowest was observed in *Chaetocnema aridula* due to light absorption by its dark pigment. The other studied species, despite their light exoskeletons, have low reflectance due to the matte texture of their covers.

Hyperspectral imaging, which covers a wider range of the electromagnetic spectrum, allows the consideration of nuances that are not visible to the naked eye. The structure of the insect's chitinous cover, its roughness, and microstructures also affect reflectance. The practical application of hyperspectral imaging requires taking into account factors such as the time of day and lighting conditions during the imaging process in order to obtain accurate and comparable data.

Thus, the results of the study expand the possibilities for applying hyperspectral imaging to the study of insect exoskeletons, which, in turn, opens new horizons for using these data in agriculture and entomology.

### **Author Contributions**

**U.R.M.** – concept and supervision of the work; **O.A.V.** – conducting the experiments; **K.M.M.** – discussion of the research results; **F.A.A.** – writing the text; **Zh.S.B.** – editing the text of the article.

### **Funding**

This research is funded by the Science Committee of the Ministry of Science and Higher Education of the Republic of Kazakhstan (Grant No. AP22784689 «Development of an integrated system for remote monitoring of spring wheat agroecosystems based on spectral imaging technology for the creation of precision agriculture»).

### **Conflict of Interest**

The authors declare no conflict of interest.

### **Compliance with ethical standards**

All procedures carried out in the studies involving animals adhered to the ethical standards of the institution where the research was conducted and complied with the legal regulations of the Republic of Kazakhstan and international organisations.

### **References**

1. Cardim Ferreira Lima M, Damascena de Almeida Leandro ME, Valero C, et al. Automatic Detection and Monitoring of Insect Pests - A Review. *Agriculture*. 2020;10(5):161. doi.org/10.3390/agriculture10050161
2. Behmann J, Mahlein A-K, Rumpf T, et al. A review of advanced machine learning methods for the detection of biotic stress in precision crop protection. *Precision Agriculture*. 2015;16(3):239-260. doi.org/10.1007/s11119-014-9372-7
3. Lacotte V, Dell'Aglio E, Peignier S, et al. A comparative study revealed hyperspectral imaging as a potential standardized tool for the analysis of cuticle tanning over insect development. *Heliyon*. 2023;9(3):e13962. doi.org/10.1016/j.heliyon.2023.e13962
4. Nansen C, Elliott N. Remote Sensing and Reflectance Profiling in Entomology. *Annual Review of Entomology*. 2016;61:139-158. doi.org/10.1146/annurev-ento-010715-023834
5. Yamada M, Thiesen LV, Iost Filho FH, Yamamoto PT. Hyperspectral imaging and machine learning: A promising tool for the early detection of *Tetranychus urticae* Koch infestation in cotton agriculture. *Agriculture*. 2024;14(9):1573. doi.org/10.3390/agriculture14091573
6. Prabhakar M, Prasad Y, Vennila S, et al. Hyperspectral indices for assessing damage by the solenopsis mealybug (Hemiptera: Pseudococcidae) in cotton. *Computers and Electronics in Agriculture*. 2013;97:61-70. doi.org/10.1016/j.compag.2013.07.004
7. Wang Y, Nansen C, Zhang Y. Integrative insect taxonomy based on morphology, mitochondrial DNA, and hyperspectral reflectance profiling. *Zoological Journal of the Linnean Society*. 2015;175(2):317-329. doi.org/10.1111/zoj.12367

8. Ferrari V, Calvini R, Boom B, et al. Evaluation of the potential of near-infrared hyperspectral imaging for monitoring the invasive brown marmorated stink bug. *Chemometrics and Intelligent Laboratory Systems*. 2023;227:104751. doi.org/10.1016/j.chemolab.2023.104751
9. Tavares GC, Silva NC. Images in red: A methodological and integrative approach for the usage of Near-infrared Hyperspectral Imaging (NIR-HSI) on collection specimens of Orthoptera (Insecta). *bioRxiv*. 2024;617997. doi.org/10.1101/2024.10.12.617997
10. Ma Z, Di M, Hu T. Visible-NIR hyperspectral imaging based on characteristic spectral distillation used for species identification of similar crickets. *Optics and Laser Technology*. 2025;183:112420. doi.org/10.1016/j.optlastec.2025.112420
11. Soltani P, Hacken M, Meijden A, et al. Polarization resolved hyperspectral imaging of the beetle *Protaetia speciosa jousseini*. *Optics Express*. 2025;33(7):14858-14871. doi.org/10.1364/OE.557318
12. Mielewicz M, Liebisch F, Walter A, et al. Near-infrared (NIR)-reflectance in insects - Phenetic studies of 181 species. *Entomological Today*. 2012;24:183-215.
13. Akin O, Kemal P. Deep Learning Applications for Hyperspectral Imaging: A Systematic Review. *Journal of the Institute of Electronics and Computer*. 2020;39-56. doi.org/10.33969/JIEC.2020.21004
14. Alt BB, Gurova TA, Elkin OV, et al. The use of Specim IQ, a hyperspectral camera, for plant analysis. *Vavilov Journal of Genetics and Breeding*. 2020;21(3):259-266. doi.org/10.18699/VJ19.587
15. Shapiro SS, Wilk MB. An analysis of variance test for normality (complete samples). *Biometrika*. 1965;52(3-4):591-611. /doi.org/10.1093/biomet/52.3-4.591
16. Levene H. Robust tests for equality of variances. In: *Contributions to Probability and Statistics*. Stanford University Press; 1960:278-292.
17. Bauriegel E, Giebel A, Geyer M, et al. Early detection of *Fusarium* infection in wheat using hyperspectral imaging. *Computers and Electronics in Agriculture*. 2011;75(2):304-312. doi.org/10.1016/j.compag.2010.12.006
18. Bravo C, Moshou D, West J, McCartney A, Ramon H. Early disease detection in wheat fields using spectral reflectance. *Biosystems Engineering*. 2003;84(2):137-145. doi.org/10.1016/S1537-5110(02)00269-6
19. Del Fiore A, Reverberi M, Ricelli A, et al. Early detection of toxigenic fungi on maize by hyperspectral imaging analysis. *International Journal of Food Microbiology*. 2010;144(1):64-71. doi.org/10.1016/j.ijfoodmicro.2010.08.001
20. Lu G, Fei B. Medical hyperspectral imaging: a review. *Journal of Biomedical Optics*. 2014;19(1):010901. doi.org/10.1117/1.JBO.19.1.010901
21. Calvini R, Ulrici A, Amigo JM. Growing applications of hyperspectral and multispectral imaging. In: Amigo JM, editor. *Data Handling in Science and Technology: Hyperspectral Imaging*. Amsterdam: Elsevier; 2019:605-629. doi.org/10.1016/b978-0-444-63977-6.00024-9
22. Chang CI. *Hyperspectral Imaging: Techniques for Spectral Detection and Classification*. New York: Kluwer; 2003:386. doi.org/10.1007/978-1-4419-9170-6
23. Lu B, Dao PD, Liu J, et al. Recent Advances of Hyperspectral Imaging Technology and Applications in Agriculture. *Remote Sensing*. 2020;12(16):2659. doi.org/10.3390/rs12162659
24. Li X, et al. Hyperspectral Imaging and Their Applications in the Nondestructive Quality Assessment of Fruits and Vegetables. In: *Hyperspectral Imaging in Agriculture, Food and Environment*. InTech; 2018:27-63. doi.org/10.5772/intechopen.72250

25. Mahlein AK, Rumpf T, Welke P, et al. Development of spectral indices for detecting and identifying plant diseases. *Remote Sensing of Environment*. 2013;128:21-30. doi.org/10.1016/j.rse.2012.09.019
26. Mirik M. Hyperspectral Spectrometry as a Means to Differentiate Uninfested and Infested Winter Wheat by Greenbug (Hemiptera: Aphididae). *Journal of Economic Entomology*. 2006;99(5):1682-1690. doi.org/10.1093/jee/99.5.1682
27. Palmquist J. Detecting Defects on Cheese using Hyperspectral Image Analysis [Master's thesis]. Umeå: Umeå University; 2020. 44. http://urn.kb.se/resolve?urn=urn:nbn:se:umu:diva-172695
28. Sarić R, Nguyen VD, Burge T, et al. Applications of hyperspectral imaging in plant phenotyping. *Trends in Plant Science*. 2022;27(3):301-315. doi.org/10.1016/j.tplants.2021.12.003
29. Soni A, Dixit Y, Reis MM, et al. Hyperspectral imaging and machine learning in food microbiology: Developments and challenges in detection of bacterial, fungal, and viral contaminants. *Comprehensive Reviews in Food Science and Food Safety*. 2022;21(5):3717-3745. doi.org/10.1111/1541-4337.12983
30. Saran S, Hiremath S, Chakraborty S, et al. Remote Sensing and Automated Monitoring Systems for Insect Pest Detection and Surveillance. *Uttar Pradesh Journal of Zoology*. 2025;46(2):155-171. doi.org/10.56557/upjoz/2025/v46i24771
31. Tamin O, Mounq EG, Dargham JA, et al. A review of hyperspectral imaging-based plastic waste detection state-of-the-arts. *International Journal of Electrical and Computer Engineering*. 2023;13(3):3407-3419. doi.org/10.11591/ijece.v13i3.pp3407-3419
32. Thomas S, Wahabzada M, Kuska MT, et al. Observation of plant-pathogen interaction by simultaneous hyperspectral imaging reflection and transmission measurements. *Functional Plant Biology*. 2017;44(1):23-34. doi.org/10.1071/FP16127
33. Vignati S, Tugnolo A, Giovenzana V, et al. Hyperspectral imaging for fresh-cut fruit and vegetable quality assessment: Basic concepts and applications. *Applied Sciences*. 2023;13(17):9740. doi.org/10.3390/app13179740
34. Wang X, Zhang M, Zhu J, Geng S. Spectral prediction of *Phytophthora infestans* infection on tomatoes using artificial neural network (ANN). *International Journal of Remote Sensing*. 2008;29(6):1693-1706. doi.org/10.1080/01431160701281007

**Гиперспектралды деректерді пайдалану арқылы жаздық бидай зиянкестерінің спектрлік сипаттамалары: диагностикасы және түсінің бейімделу ерекшеліктері**

**Р.М. Уалиева\*<sup>1</sup>, А.В. Осипова<sup>1</sup>, М.М. Каверина<sup>1</sup>, А.А. Фаурат<sup>1</sup>, С.Б. Жангазин<sup>2</sup>**

<sup>1</sup>*Торайғыров университеті, Павлодар, Қазақстан*

<sup>2</sup>*Л.Н. Гумилев атындағы Еуразия ұлттық университеті, Астана, Қазақстан*

**Аңдатпа.** Гиперспектралды түсіруді пайдалана отырып, солтүстік-шығыс Қазақстанда жаздық бидаймен байланысты алты зиянкес түрінің (*Chorosoma schillingii*, *Loxostege sticticalis*, *Tettigonia viridissima*, *Chaetocnema aridula*, *Calliptamus italicus* және *Laodelphax striatella*) спектрлік сипаттамалары алғаш рет зерттелді. Бұл зерттеу осы тақырып бойынша бар болғаны бірнеше ғылыми еңбектерді толықтырады. Спектрлерді талдау жәндіктердің жарықты қалай шағылыстыратынын, беретінін және сіңіретінін көрсетті, бұл осы деректерді егістіктердегі зиянкестерді айырып тану тапсырмаларында одан әрі қолдануға мүмкіндік береді. Зерттелген



түрлердің спектрі 500-780 нм аралығында болады. Жоғары шағылысу жәндіктер денесінің жеңіл және тегіс аймақтарына тән, ал қараңғы, біркелкі емес және кедір-бұдырлы бөліктер жарықты шашыратып, жалпы шағылыстыруды төмендетеді. Зерттелген үлгілердің ішінде ең жоғары шағылысу қабілеті *Chorosoma schillingii* түрінің үлгісінде тегіс құрылым мен жабындардың ашық түсінің үйлесуіне байланысты байқалады. Бұл сондай-ақ жақын инфрақызыл спектріндегі қарқынды шағылысумен байланысты. Ең төменгі шағылысу коэффициенті *Chaetocnema aridula* түрінде тіркелген, бұл оның қара пигментімен жарықты сіңірумен түсіндіріледі. Көптеген басқа түрлердің ашық түсті экзоскелетіне қарамастан, олардың шағылысу коэффициенті жабындардың күңгірт құрылымына байланысты төмен болып қалады. Жәндіктердің түсі тек өсімдік фонында жасыруға көмектесіп қана қоймай, сонымен қатар қоршаған орта жағдайларына бейімделу болуы мүмкін. Ашық түстер күн сәулесін шағылыстыруға көмектесіп, артық қызып кетуден қорғайды, ал қара түстер ультракүлгін сәулесінен қорғаныс ролін атқаруы мүмкін. Жәндіктердің дене бөліктерінің әр түрлі түстері болуы мүмкін, бұл экологиялық жағдайларға функционалды бейімделумен байланысты.

**Түйін сөздер:** гиперспектралды визуализация, спектрлік сипаттамалар, энтомофауна, бидай агроценозы, зиянкестер

### **Спектральные характеристики вредителей яровой пшеницы с использованием гиперспектральных данных: диагностика и адаптационные особенности окраса**

**Р.М. Уалиева\*<sup>1</sup>, А.В. Осипова<sup>1</sup>, М.М. Каверина<sup>1</sup>, А.А. Фаурат<sup>1</sup>, С.Б. Жангазин<sup>2</sup>**

<sup>1</sup>Торайгыров университет, Павлодар, Казахстан

<sup>2</sup>Евразийский национальный университет им. Л.Н. Гумилева, Астана, Казахстан

**Аннотация.** С использованием гиперспектральной съемки впервые были исследованы спектральные характеристики шести видов вредителей (*Chorosoma schillingii*, *Loxostege sticticalis*, *Tettigonia viridissima*, *Chaetocnema aridula*, *Calliptamus italicus* и *Laodelphax striatella*), связанных с яровой пшеницей в северо-восточном Казахстане, что дополняет немногочисленные существующие исследования по данной теме. Анализ спектров показал, как насекомые отражают, передают и поглощают свет, что открывает возможности для дальнейшего применения этих данных в задачах распознавания вредителей на полях. Исследованные виды имеют диапазон спектра в пределах 500-780 нм. Высокий коэффициент отражения характерен для светлых и гладких участков тела насекомых, в то время как темные, неровные и шероховатые части рассеивают свет, снижая общую отражательную способность. Среди исследованных образцов наиболее высокая отражательная способность наблюдается у экземпляра вида *Chorosoma schillingii* благодаря сочетанию гладкой структуры и светлого окраса покровов. Это также связано с интенсивным отражением в ближнем инфракрасном спектре. Наименьший коэффициент отражения зафиксирован у *Chaetocnema aridula*, что объясняется поглощением света темным пигментом. Несмотря на светлый экзоскелет у большинства других видов, их коэффициент отражения остается низким из-за матовой текстуры покровов. Цветовое окрашивание насекомых не только способствует маскировке на растительном фоне, но также может быть адаптацией к условиям окружающей среды. Светлая окраска способствует отражению солнечного

света и предотвращает перегрев, в то время как темная окраска может служить защитой от ультрафиолетового излучения. Разные части тела насекомых могут иметь различные окраски, что связано с функциональными адаптациями к экологическим условиям.

**Ключевые слова:** гиперспектральная визуализация, спектральные характеристики, энтомофауна, агроценоз пшеницы, вредители

#### **Сведения об авторах:**

**Уалиева Римма Мейрамовна** – автор-корреспондент, PhD, профессор кафедры «Биология и экология», НАО «Торайгыров университет», ул. Ломова 64, 140008, Павлодар, Казахстан.

**Осипова Анастасия Вячеславовна** – студент бакалавриата, кафедра «Биология и экология», НАО «Торайгыров университет», ул. Ломова 64, 140008, Павлодар, Казахстан.

**Каверина Мария Михайловна** – докторант кафедры «Биология и экология», НАО «Торайгыров университет», ул. Ломова 64, 140008, Павлодар, Казахстан.

**Фаурат Алина Александровна** – PhD, ассоциированный профессор кафедры «География и туризм», НАО «Торайгыров университет», ул. Ломова 64, 140008, Павлодар, Казахстан.

**Жангазин Саян Берикович** – PhD, ассоциированный профессор, заместитель декана по научной работе факультета естественных наук, НАО «Евразийский национальный университет им. Л.Н. Гумилева», Казымукан 13, 010000, Астана, Казахстан.

#### **Авторлар туралы мәліметтер:**

**Уалиева Римма Мейрамовна** – хат-хабар авторы, PhD, «биология және экология» кафедрасының профессоры, «Торайгыров университеті» КеАҚ, Ломов көшесі, 64, 140008, Павлодар, Қазақстан.

**Осипова Анастасия Вячеславовна** – бакалавриат студенті, «биология және экология» кафедрасы, «Торайгыров университеті» КеАҚ, Ломов көшесі, 64, 140008, Павлодар, Қазақстан.

**Каверина Мария Михайловна** – «биология және экология» кафедрасының докторанты, «Торайгыров университеті» КеАҚ, Ломов көшесі, 64, 140008, Павлодар, Қазақстан.

**Фаурат Алина Александровна** – PhD, «география және туризм» кафедрасының қауымдастырылған профессоры, «Торайгыров университеті» КеАҚ, Ломов көшесі, 64, 140008, Павлодар, Қазақстан.

**Жангазин Саян Берикович** – PhD, қауымдастырылған профессор, жаратылыстану ғылымдары факультеті деканының ғылыми жұмыс жөніндегі орынбасары, «Л.Н. Гумилев атындағы Еуразия ұлттық университеті» КеАҚ, Қажымұқан 13, 010000, Астана, Қазақстан.

#### **Authors' information:**

**Ualiyeva Rimma Meyramovna** – Corresponding author, PhD, Professor, Department of Biology and Ecology, Toraighyrov University, 64 Lomov St., 140008, Pavlodar, Kazakhstan.

**Osipova Anastasiya Vyacheslavovna** – Bachelor's degree student, Department of Biology and Ecology, Toraighyrov University, 64 Lomov St., 140008, Pavlodar, Kazakhstan.

**Kaverina Mariya Mikhailovna** – PhD student, Department of Biology and Ecology, Toraighyrov University, 64 Lomov St., 140008, Pavlodar, Kazakhstan.

**Faurat Alina Aleksandrovna** – PhD, Associate Professor, Department of Geography and Tourism, Toraighyrov University, 64 Lomov St., 140008, Pavlodar, Kazakhstan.

**Zhangazin Sayan Berikovich** – PhD, Associate Professor, Deputy Dean for Research of the Faculty of Natural Sciences, L.N. Gumilyov Eurasian National University, Khadzhimukan 13, 010000, Astana, Kazakhstan.